doi.org/10.62683/SINARG2025.229

Research paper

PHOTOMETRIC ANALYSIS OF HOMOGENIZED X-RAY IMAGES IN DETERMINING THE MECHANICAL PROPERTIES OF WOOD: PRELIMINARY RESULTS

Andrej Josifovski[1], Irina Živković[2], Nebojša Todorović[3], Marko Veizović[4], Jelena Milošević[5], Aleksandar Rajčić[6]

Abstract

Previous research demonstrated a link between wood strength and brightness intensity in X-ray images. Wood samples were subjected to compression testing along and across the grain, with X-ray imaging performed on the same specimens before the mechanical tests. Differences in the brightness of X-ray images of test specimens were clearly noticeable, both in relation to the type of sampled wood and depending on the specific alignment of X-ray beams relative to the direction of wood fibers in the test specimen. Because wood has an anisotropic structural composition, it is expected that the X-ray image of the tested sample would exhibit uneven brightness. Photometric analysis of the X-ray image using computer software allows for assigning appropriate mechanical properties to each point on the image via x, y, v parameters. However, since an individual light point cannot represent the cumulative mechanical properties of the sampled test specimen, it is clear that the task at hand also includes the need for homogenizing the X-ray image. This is achievable through the program's three-dimensional approximation capabilities. The creation of a tonal grayscale through image homogenization would enable the alignment of mechanical strength parameters with brightness intensity values. This process would effectively represent the overall mechanical potential of the wood sample as a cumulative result, linking the homogenized brightness of the X-ray image with the wood's strength characteristics.

Key words: *Photometric, X-ray, OsiriX, Tonal gray scale, Equalization, Wood*

[1] PhD, Assistant Professor, Faculty of Architecture – University of Belgrade, Belgrade, Serbia, andrej@arh.bg.ac.rs , [0000-0002-7390-9579]

[2] Teaching assistant and PhD student, Faculty of Architecture – University of Belgrade, Belgrade, Serbia, irina.zivkovic@arh.bg.ac.rs, [0009-0009-2817-6220]

[3] PhD, Professor, Faculty of Forestry – University of Belgrade, Belgrade, Serbia, nebojsa.todorovic@sfb.bg.ac.rs , [0000-0002-5270-9789]

[4] Teaching assistant and PhD student, Faculty of Forestry – University of Belgrade, Belgrade, Serbia, marko.veizovic@sfb.bg.ac.rs, [0000-0002-3099-2368]

[5] PhD, Assistant Professor, Faculty of Architecture – University of Belgrade, Belgrade, Serbia, jelena@arh.bg.ac.rs , [0000-0001-7293-8194]

[6] PhD, Associate Professor, Faculty of Architecture – University of Belgrade, Belgrade, Serbia, rajcic@arh.bg.ac.rs , [0000-0003-0156-0061]

1. INTRODUCTION

The concept for this research arose from the necessity of restoring wooden structures in architectural objects of cultural and historical significance, where such work is governed by specific regulations that require a specialized, non-invasive diagnostic approach. This methodological framework is also recommended for the restoration and reconstruction of other structures of potential heritage value, as each may be regarded as a monument to the era in which it was created. The procedures for such restoration efforts are outlined in a document adopted by ICOMOS during the General Assembly held in New Delhi in 2017. This document details the principles for the conservation of wooden architectural heritage, emphasizing the protection of their authenticity and structural integrity [1, 2].

Identifying the most stressed points of the structure and detecting signs of degradation and damage in wood are essential prerequisites for developing an appropriate rehabilitation plan. The non-destructive nature of the diagnostic process necessitates in situ examination. Therefore, this study aimed to establish a reliable and easily applicable non-destructive diagnostic method. The use of X-rays was considered for this purpose, as their orientation can be aligned either parallel or perpendicular to the wood grain, analogous to laboratory-based static mechanical testing [3, 4].

In our previous research involving X-ray application, tabulated strength values of experimental wood samples were used, and it was confirmed that samples with higher strength yielded brighter X-ray images, validating the analogy. The harmonization of mechanical and radiographic parameters now required standardized mechanical calibration of the wood specimens and computerized objectification of image brightness. This methodology was supported by the capabilities of the OsiriX software, indicating its suitability for the intended analysis [5, 6].

2. METHODOLOGY

X-ray testing was conducted on wood samples from diffuse-porous hardwoods—beech (Fagus sylvatica) and poplar (Populus spp.); ring-porous hardwoods—black locust (Robinia pseudoacacia) and oak (Quercus spp.); and softwoods—pine (Pinus spp.) and silver fir (Abies alba), including a control group of samples from horse chestnut (Aesculus hippocastanum). To ensure X-ray image homogenization, the specimens were cut to dimensions of 20 × 20 × 40 mm. These samples were prepared similarly to those used in standard compressive strength tests, with the longitudinal axis aligned with the grain direction. The longitudinal plane intersecting the sample perpendicularly to its length was parallel to the grain lines and considered the axial plane, while the planes intersecting the two longitudinal sides at right angles represented the tangential and radial planes [4, 7, 8].

A second set of specimens had a transverse profile, with the axial plane intersecting the longest dimension at a right angle. Testing was carried out using a medical-grade X-ray machine operating within a range of 40–125 kV and 0.50–360 mA/s, similar to those used in clinical diagnostics, where upper limits are typically 100 kV and 70 mA/s. Each sample set was imaged using a current voltage of 37 kV and a strength of 70 mA/s. Following radiography, standard compressive strength testing was also performed on the same specimens.

The brightest X-ray images were observed in the ring-porous hardwoods, which also exhibited the highest measured compressive strength. Progressively lower brightness was observed in the diffuse-porous hardwoods, with the lowest intensity seen in the softwood samples. The brightest images in all test groups were obtained when X-rays were directed along the axial plane; lower brightness was noted when X-rays were directed in the radial direction, and the lowest when directed tangentially, corresponding proportionally to the measured compressive strengths [9, 10, 11] (see Appendix).

3. RESULTS

3.1. Photometric Analysis:

Photometric analysis of the X-ray images represented the final step in the harmonization of mechanical and radiographic parameters. This was performed using OsiriX software, which is widely used in medical diagnostics. Its three main operational components—Database Window, Viewer Window, and 3D Volume Rendering—enable the importation of X-ray datasets, 2D/3D image viewing, and image manipulation within the study list environment [6, 11, 12].

Of particular importance is the drop-down menu tool *WW/WL* (Window Width/Window Level), used to adjust image brightness and contrast. The software's CLUT (Color Look-Up Table) module offers additional tools for selecting and adjusting color ranges, which can enhance operational precision.

Due to the heterogeneous and anisotropic nature of wood—where mechanical properties vary according to the direction of grain flow, leading to image brightness variability—the software tools especially valuable for structural wood visualization include *Orientation* (for spatial positioning relative to horizontal, frontal, and sagittal planes) and *Thick Slab* (for deepening cross-sectional views) [13].

Key tools for image homogenization and analysis include:

- **ROI Tools** (Region of Interest): Enable targeted image analysis.
- **Repulsor Tool**: For manipulating defined ROIs.
- **Selector Tool**: Allows grayscale and color adjustments within selected ROIs.
- **Propagate Tool**: Applies defined ROIs across all cross-sections.
- **Region Growing**: Expands areas around selected points, useful for diagnosing damage and degradation in structural wood elements.
- **Filters**, particularly **Convolution Filters** in the 2D Viewer menu, used in bone diagnostics, offer potential applicability here by producing 3D renderings with enhanced contrast.

The **3D Volume Rendering** module enables each point in the image to be assigned corresponding mechanical properties based on its x, y, z coordinates. However, due to the anisotropic nature of wood, a single point cannot fully represent the collective mechanical properties of the entire specimen, even though dimensional uniformity helps in achieving a certain level of homogenization.

Therefore, X-ray image brightness homogenization must ultimately rely on additional operational tools such as **Engine Tools**, which support Ray Cast and 3D Texture applications.

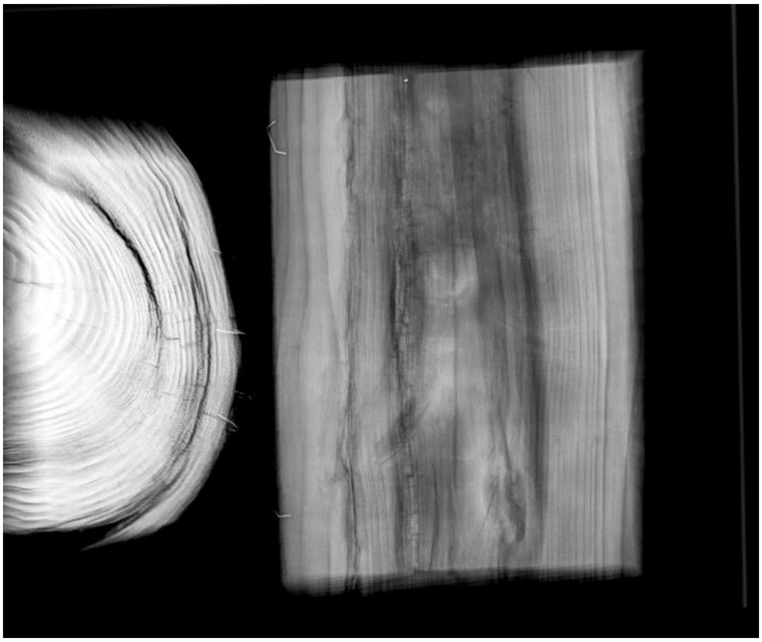

Figure 1. X-ray of a log of wood

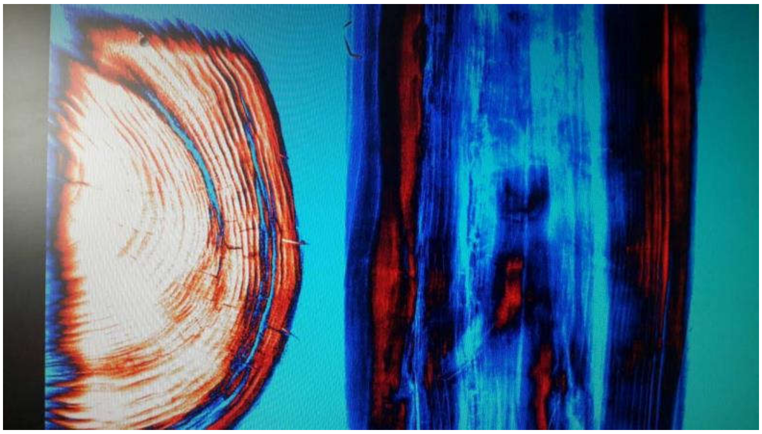

Figure 2. X-ray image through OsiriX software - example

4. CONCLUSION

The harmonization of mechanical and photometric parameters should result from a comprehensive evaluation of the material's mechanical properties.This approach significantly enhances the diagnostic reliability and practical value of the material evaluation process. Future work could focus on refining this diagnostic method for larger structural elements and validating it through in situ testing.

ACKNOWLEDGMENTS

This research was funded by the Ministry of Education, Science and Technological Development of the Republic Serbia, grant number 451-03-68/2020-14/200090. The research was done under the research units of the University of Belgrade – Faculty of Architecture, Laboratory for Innovative Structures in Architecture (LISA).

REFERENCES

[1] Avdelidis, N.P., Moropoulou, A. **Applications of Infrared Thermography for the Investigation of historic structures**. *J. Cult. Herit.* 2004, *5*, 119–127. https://doi.org/10.1016/j.culher.2003.07.002.

[2] Hussain, A.; Akhtar, S. **Review of Non-Destructive Tests for Evaluation of Historic Masonry and Concrete Structures**. *Arab. J. Sci. Eng.* 2017, *42*, 925–940. https://doi.org/10.1007/s13369-017-2437-y

[3] Bucur, V.; Böhnke, I. **Factors affecting ultrasonic measurements in solid wood**. *Ultrasonics* 1994, *32*, 385–390. https://doi.org/10.1016/0041-624X(94)90109-0.

[4] Fais, S.; Casula, G.; Cuccuru, F.; Ligas, P.; Bianchi, M.G. **An innovative methodology for the non-destructive diagnosis of architectural elements of ancient historical buildings**. *Sci. Rep.* 2018, *8*, 4334. https://doi.org/10.1038/s41598-018-22601-5

[5] Barnaure, M.; Cincu, M. **Testing methods for the assessment of material properties in historical masonry structures: A review**. *Proc. IOP Conf. Ser.: Mater. Sci. Eng.* 2019, *662*, 032040. https://doi.org/10.1088/1757-899x/789/1/012003.

[6] Josifovski, A; Savanović, D. **Non-destructive testing of wood structures by x-rays**. *SAJ,* 2017, *1,* 51–64.

[7] Martinez, I.; Martinez, E. **Qualitative Timber Structure Assessment with Passive IR Thermography. Case Study of Source of Common Errors**. *Case Stud. Constr. Mater.* **2022**, *16*, e00789. https://doi.org/10.1016/j.cscm.2021.e00789.

[8] Pentoney R.E.; Davidson. R.W. **Rheology and the study of wood**. *Forest. Pro. J.* 1962, *12*, 243–248.

[9] Nowak, T.P.; Jasieńko, J.; Hamrol-Bielecka, K. **In situ assessment of structural timber using the resistance drilling method—Evaluation of usefulness**. *Constr. Build. Mater.* 2016, *102*, 403–415. https://doi.org/10.1016/j.conbuildmat.2015.

[10] Wang, P.; Li, S.; Macchioni, N.; Palanti, S.; Milani, G. **Comprehensive Evaluation Method of Historical Timber Structural Building Taking Fujiu Zhou House as an Example**. *Forests* 2021, *12*, 1172. https://doi.org/10.3390/f12091172.

[11] Nasir, V.; Ayanleye, S.; Kazemirad, S.; Sassan, F.; Adamopoulos, S. **Acoustic Emission Monitoring of Wood Materials and Timber Structures: A Critical Review**. *Build. Mater.* 2022, *350*, 12887. https://doi.org/10.1016/j.conbuildmat.2022.128877.

[12] Xin, Z., Ke, D.; Zhang, H.; Yu, Y.; Liu, F. **Non-destructive Evaluating the Density and Mechanical Properties of Ancient Timber Members Based on Machine Learning Approach**. *Build. Mater.* 2022, *341*, 127855. https://doi.org/10.1016/j.conbuildmat.2022.127855

[13] Šoškić, B.; Popović, Z. **Svojstva Drveta**; *Šumarski Fakultet Univerziteta*: Belgrade, Serbia, 2002; p. 32.

APPENDIX

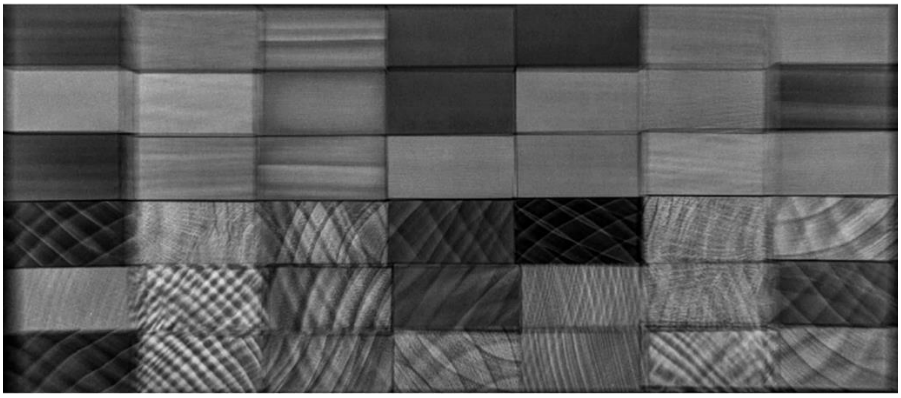

Figure 3. Mosaic.

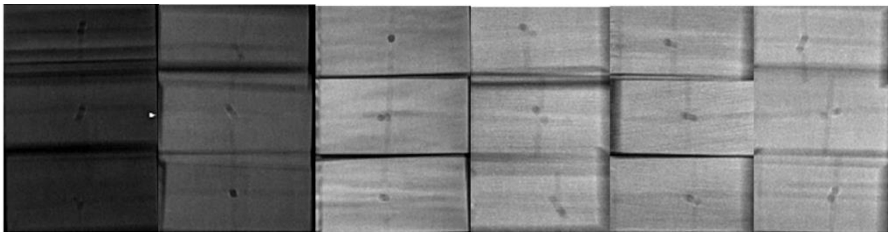

Figure 4. Zebra.

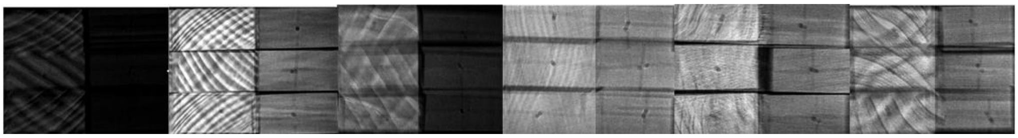

Figure 5. Tonal palette.

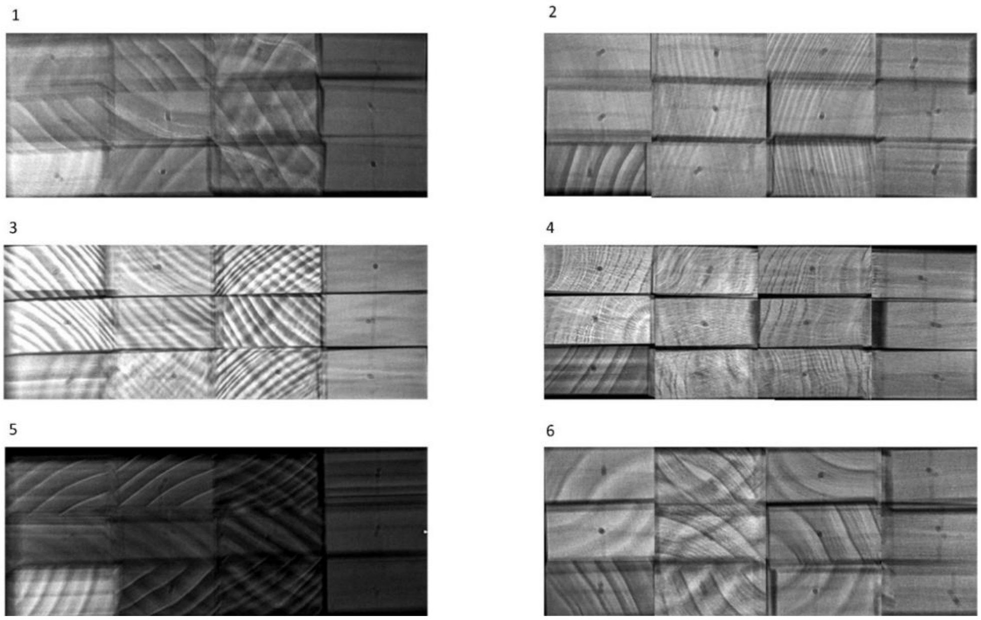

Figure 5. Wood samples. 1.poplar; 2 beech; 3 pine; 4.oak; 5.fir; 6. acacia.

Table 1. Values of compressive stresses determined on test sample in the calibration procedure of the stress-sound wave application method.

	Softwood					Hardwood					
						Ring Porous				Diffuse Porous	
	Spruce 1	**Fir 1**	**Fir 2**	**Pine 1**	**Pine 2**	**Oak 1**	**Oak 2**	**Black Locust1**	**Black Locust2**	**Beech 1**	**Beech 2**
Length (mm)	39.72	40.2	39.13	39.37	39.1	39.04	39.3	39.32	39.3	39.48	39.57
Width (mm)	20.18	20.16	19.96	20.12	19.93	19.92	19.86	19.79	20.27	19.94	19.8
Thickness	/	/	/	/	/	/	/	/	/	/	/
Compressive force—transversal (lateral)	3113	1883	1648	13129	4979	4149	4621	5839	4736	4624	4760
Compressive force—axial (transverse)	/	/	/	/	/	/	/	/	/	/	/
Transversal stress	3.9	2.3	2.1	16.6	6.4	5.3	5.9	7.5	5.9	5.9	6.0
Axial stress	/	/	/	/	/	/	/	/	/	/	/
Length (mm)	/	/	/	/	/	/	/	/	/	/	/
Width (mm)	19.75	10.86	19.94	20.08	20.29	19.84	19.84	19.93	20.02	19.82	19.96
Thickness	19.86	19.85	19.89	20.09	20.08	19.77	19.79	19.9	20.12	19.19	19.9
Compressive force—transversal (lateral)	/	/	/	/	/	/	/	/	/	/	/
Compressive force—axial (transverse)	19,550	2116	21,212	34,214	27,739	24,223	27,742	39,241	37,842	31,563	29,053
Transversal stress	/	/	/	/	/	/	/	/	/	/	/

Table 2. Values of bending stress determined on test samples in the calibration procedure of the stress sound wave application method.

	Softwood					Hardwood					
						Ring Porous				Diffuse Porous	
	Spruce 1	Fir 1	Fir 2	Pine 1	Pine 2	Oak 1	Oak 2	Black Locust1	Black Locust Acacia 2	Beech 1	Beech 2
h [mm]	19.74	19.86	19.84	20.01	19.78	19.89	19.85	19.79	20.1	19.88	19.91
b [mm]	19.72	19.83	19.88	20.11	19.91	19.88	19.84	19.94	20.06	19.92	19.81
Bending strength MPa [N/mm^2]	88.9	79.9	71.6	132.9	102.8	91.09	124.5	86.4	170.3	169.8	128
Modulus of elasticity MPa [N/mm^2]	6108	8137	7905	11567	7448	6792	8232	11020	14788	11987	9145
Force max. [N]	1627	1488	1334	2572	1907	1706	2316	1605	3288	3182	2393
Deflection max. [mm]	13.85	11.78	10.28	9.39	17.95	16.58	15.04	10.27	14.5	12.64	16.67
h [mm]	19.74	19.83	19.89	19.98	20.03	19.85	19.94	19.9	10.07	19.9	19.8
b [mm]	19.78	19.79	19.86	19.92	20.14	19.83	19.85	19.92	20.31	19.84	19.8
Bending strength MPa [N/mm^2]	84.1	81.3	76.9	152.1	119.1	103.3	105.8	200.9	185.2	135.9	133.3
Modulus of elasticity MPa [N/mm^2]	8784	8262	7304	12,778	10,337	7722	6882	15,175	13,920	10,315	9722
Force max. [N]	1544	1506	1438	2880	2291	1921	1987	3773	3607	2542	2464
Deflection max. [mm]	12.58	11.26	11.06	18.21	12.6	17.36	20.05	13.16	14.74	11.61	12.59